Figure S1

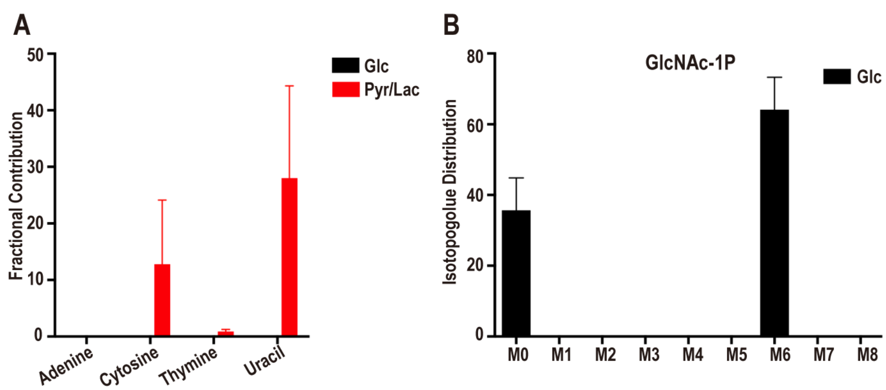
A
B
50
40
30
20
10
0
Fractional Contribution
Adenine
Cytosine
Thymine
Uracil
Glc
Pyr/Lac
GlcNAc-1P
80
60
40
20
0
Isotopogolue Distribution
M0
M1
M2
M3
M4
M5
M6
M7
M8
Glc

Figure S2

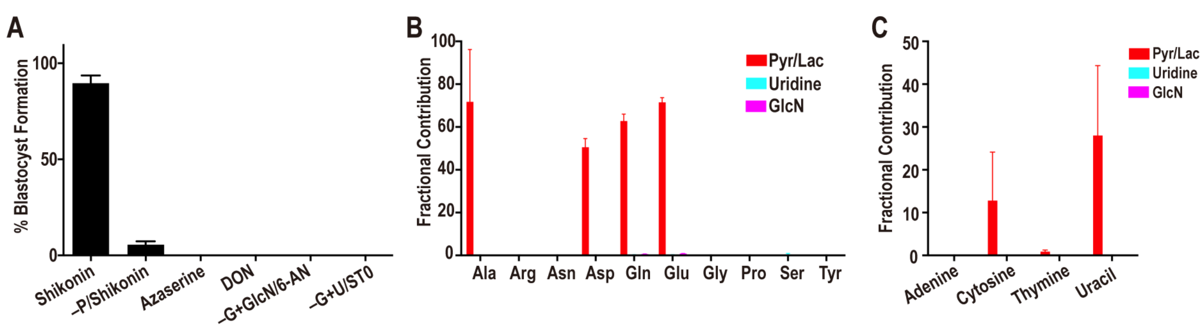
A
% Blastocyst Formation
100
50
0
Shikonin
–P/Shikonin
Azaserine
DON
–G+GlcN/6-AN
–G+U/ST0
B
Fractional Contribution
100
80
60
40
20
0
Ala
Arg
Asn
Asp
Gln
Glu
Gly
Pro
Ser
Tyr
Pyr/Lac
Uridine
GlcN
C
Fractional Contribution
50
40
30
20
10
0
Adenine
Cytosine
Thymine
Uracil
Pyr/Lac
Uridine
GlcN

Fig S3

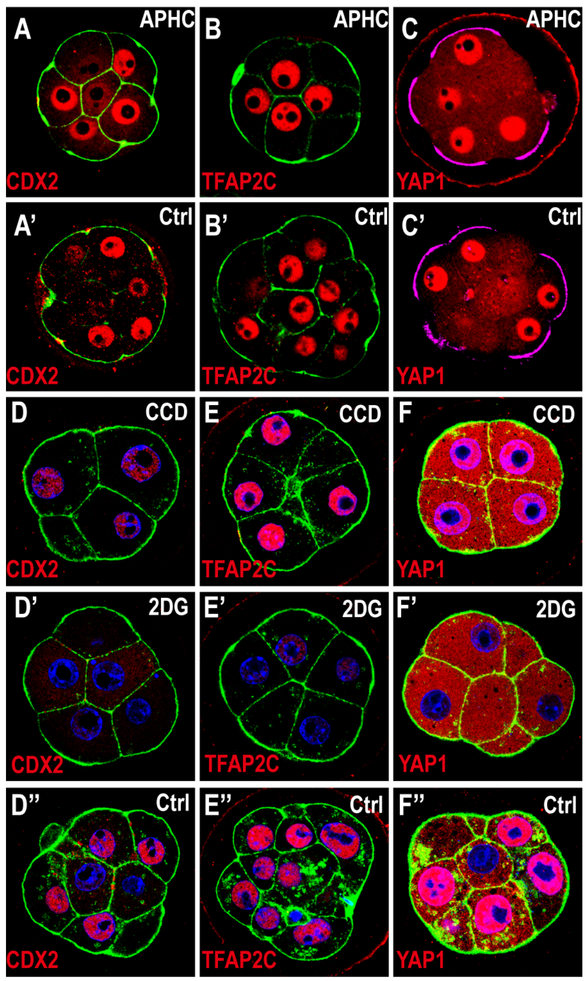

A
APHC
CDX2
B
APHC
TFAP2C
C
APHC
YAP1
A'
Ctrl
CDX2
B'
Ctrl
TFAP2C
C'
Ctrl
YAP1
D
CCD
CDX2
E
CCD
TFAP2C
F
CCD
YAP1
D'
2DG
CDX2
E'
2DG
TFAP2C
F'
2DG
YAP1
D''
Ctrl
CDX2
E''
Ctrl
TFAP2C
F''
Ctrl
YAP1

Figure S4

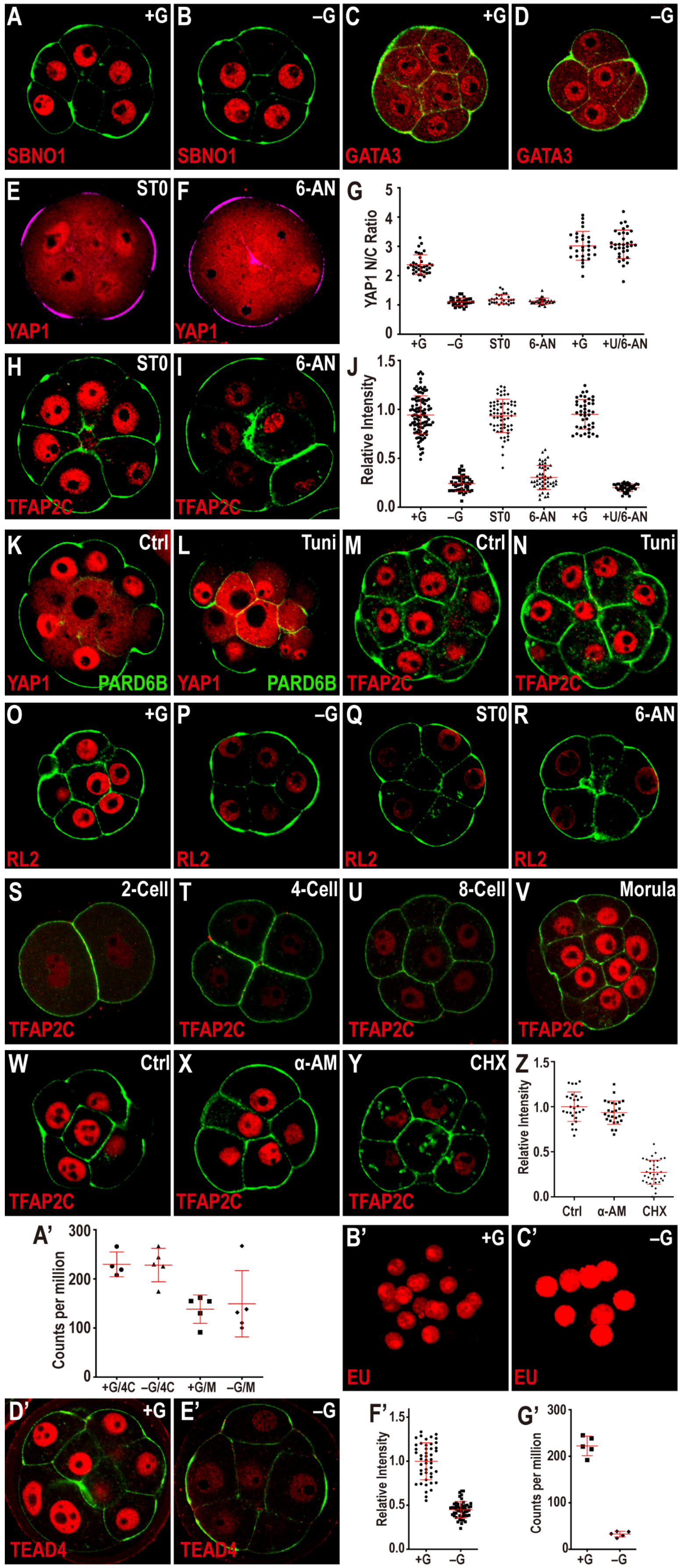

A +G
B –G
C +G
D –G
SBNO1
SBNO1
GATA3
GATA3
E ST0
F 6-AN
G
YAP1
YAP1
YAP1 N/C Ratio
+G –G ST0 6-AN +G +U/6-AN
H ST0
I 6-AN
J
TFAP2C
TFAP2C
Relative Intensity
+G –G ST0 6-AN +G +U/6-AN
K Ctrl
L Tuni
M Ctrl
N Tuni
YAP1 PARD6B
YAP1 PARD6B
TFAP2C
TFAP2C
O +G
P –G
Q ST0
R 6-AN
RL2
RL2
RL2
RL2
S 2-Cell
T 4-Cell
U 8-Cell
V Morula
TFAP2C
TFAP2C
TFAP2C
TFAP2C
W Ctrl
X α-AM
Y CHX
Z
TFAP2C
TFAP2C
TFAP2C
Relative Intensity
Ctrl α-AM CHX
A'
Counts per million
+G/4C –G/4C +G/M –G/M
B' +G
C' –G
EU
EU
D' +G
E' –G
TEAD4
TEAD4
F'
Relative Intensity
+G –G
G'
Counts per million
+G –G

Figure S5

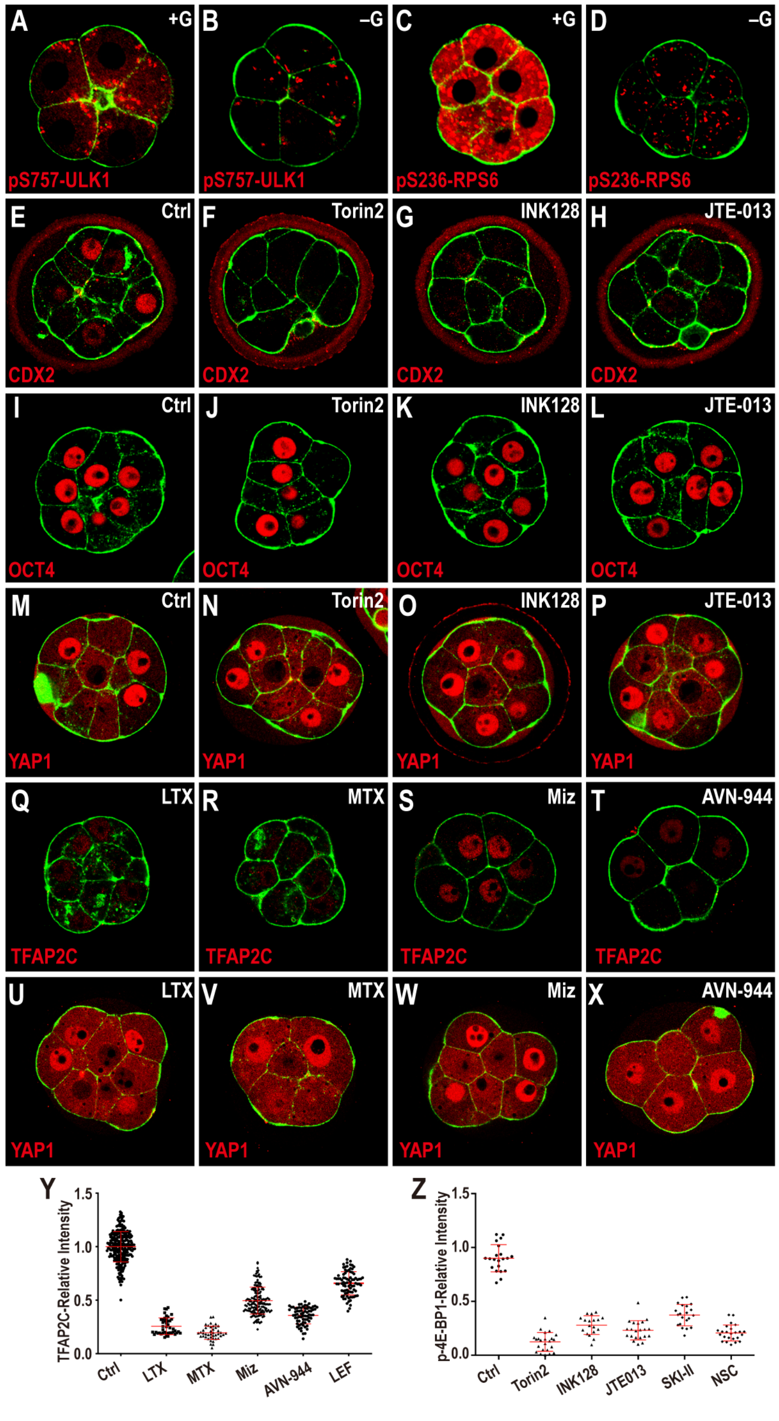

A +G pS757-ULK1
B –G pS757-ULK1
C +G pS236-RPS6
D –G pS236-RPS6
E Ctrl CDX2
F Torin2 CDX2
G INK128 CDX2
H JTE-013 CDX2
I Ctrl OCT4
J Torin2 OCT4
K INK128 OCT4
L JTE-013 OCT4
M Ctrl YAP1
N Torin2 YAP1
O INK128 YAP1
P JTE-013 YAP1
Q LTX TFAP2C
R MTX TFAP2C
S Miz TFAP2C
T AVN-944 TFAP2C
U LTX YAP1
V MTX YAP1
W Miz YAP1
X AVN-944 YAP1
Y
TFAP2C-Relative Intensity
1.5
1.0
0.5
0.0
Ctrl
LTX
MTX
Miz
AVN-944
LEF
Z
p-4E-BP1-Relative Intensity
1.5
1.0
0.5
0.0
Ctrl
Torin2
INK128
JTE013
SKI-II
NSC

Supplementary Figure Legends

Figure S1. Metabolomic analysis of the compacted morula, related to Figure 2.

(**A**) Contribution of glucose and pyruvate/lactate to nucleobases. U-^{13}C-glucose does not contribute carbon to either the purine bases (adenine) or to the pyrimidine bases (cytosine, uracil). In contrast, U-^{13}C-pyruvate/lactate contribute to the pyrimidines, but not the purine bases. The nucleobases are generated from the breakdown of nucleotides, and their labeling pattern is an indirect read-out of the labeling of bases within the nucleotides.

(**B**) U-^{13}C-glucose isotopologue distribution of HBP related metabolite GlcNAc-1P. The most abundant isotopologue is M6 in which 6 of the donated carbons are from exogenous (^{13}C) glucose. M0 peak corresponds to unlabeled metabolites from internal resources.

Figure S2. Metabolic contribution of glycolysis, PPP and HBP, related to Figure 3.

(**A**) Percentage of embryos that form blastocysts when cultured with added inhibitors or nutrient supplements. Inhibition of glycolysis (PKM2) by shikonin in +G has no adverse effect on blastocyst formation. However, in the absence of pyruvate (+G–P), shikonin blocks blastocyst formation. Inhibition of HBP by azaserine, or DON, both block the morula to blastocyst transition. Embryos cultured in medium containing GlcN in place of glucose remain sensitive to inhibition of the PPP by 6-AN. Uridine (U) does not rescue a block caused by inhibition of OGT by ST045849 (ST0).

(**B**) Metabolomic analysis shows that, unlike pyruvate/lactate (red), uridine (light blue) and GlcN (purple) do not contribute carbons to non-essential amino acids.

(**C**) As seen with glucose, labeled uridine and GlcN do not contribute carbon to nucleobase biosynthesis. In contrast, labeled pyruvate/lactate contribute carbon to pyrimidine base biosynthesis.

Figure S3. TE fate defect is not caused by 8-cell block, related to Figures 4 and 5.

Cell membranes (green) are marked using phalloidin-FITC (**A, A', B, B', D-F'**), and apical surface (purple) are marked by pERM (**C, C'**). Aphidicolin (APHC) was added to the embryos at the early 8-cell stage (66h) to inhibit the DNA synthesis and cell cycle progression (**A-C**). Cytochalasin D (CCD) was added to the embryos to inhibit cleavage (**D-F**).

At 78h control embryos are 8-16 cells and CDX2 (red) is expressed in the polar cells (**A', D''**).

APHC (**A**) and CCD (**D**) treated embryos are arrested at the 8-cell stage (78h), but have high levels of CDX2 expression.

APHC (**B**) and CCD (**E**) treated embryos have high levels of TFAP2C (red) that is similar to that seen in control embryos (**B', E''**).

YAP1 nuclear localization (red) in APHC (**C**) and CCD (**F**) treated embryos is similar to that seen in the polar cells of control embryos (**C', F''**).

(**D'-F'**) CDX2, TFAP2C and YAP1 are disrupted upon 2DG treatment.

Figure S4. Glucose dependent activation of transcription factors, related to Figure 5.

Cell membranes (green) are marked using phalloidin-FITC, and apical surface are marked by pERM (purple in **E, F**) or PARD6B (green in **K, L**).

(**A-D**) Expression of SBNO1 (**A, B**) or GATA3 (**C, D**) in morula stage (78h) embryos is not dependent on exogenously provided glucose.

(**E-G**) PPP/HBP and YAP1 nuclear localization at compacted 8-cell stage (74h). In +G control (see Figure 5A) YAP1 is localized to the nucleus in pERM (purple) marked polar cells. Inhibition of *O*-glycosylation by ST045849 (**E**) or PPP by 6-AN (**F**) both give results similar to that of –G (see Figure 5B). (**G**) Quantitation of YAP1 nuclear to cytoplasmic (N/C) ratio at 74h, YAP1 data set at morula stage (78h) in Figure 5O, 5Q are also included.

(**H-J**) In control medium TFAP2C (red) is expressed in the nuclei of all blastomeres at morula stage (78h) (see Figure 5D). This expression is insensitive to *O*-linked glycosylation inhibition by ST045849 (**H**), but is lost when the PPP is inhibited by 6-AN (**I**). Quantitation shown in (**J**), TFAP2C quantitation in Figure 5R, 5T are also included.

(**K-N**) *N*-linked glycosylation and TE specification. Apical cells with high levels of PARD6B (green) on their membrane also show nuclear localization of YAP1 (red) (**K**). Blocking *N*-glycosylation by tunicamycin (Tuni) treatment causes partial disruption in PARD6B apical localization (**L**). Apical cells that have lost apical PARD6B do not express YAP1 in the nucleus, but in other apical cells that maintain PARD6B expression YAP1 is localized in the nucleus (**L**). Tunicamycin treatment (**N**) does not influence the expression of TFAP2C (**M, N**).

(**O-R**) *O*-linked glycosylation is glucose, HBP and PPP dependent. *O*-linked glycosylation is detected using the RL2 antibody and decreases in embryos grown without glucose (**P**), or when *O*-linked glycosylation is inhibited by ST045849 (**Q**), or when the PPP is inhibited using 6-AN (**R**).

(**S-V**) TFAP2C expression during preimplantation development. TFAP2C expression is low at the 2-cell (**S**), 4-cell (**T**), and early 8-cell (**U**) stages, and then increases at the compacted morula (**V**) stage.
(**W-Z**) TFAP2C expression is sensitive to inhibition of translation. Blocking translation by cycloheximide (CHX) (**Y**), but not transcription inhibition by α-amanitin (α-AM) (**X**) causes a reduction in nuclear TFAP2C levels. (**Z**) Quantitation of nuclear TFAP2C.

(**A'**) *Tfap2c* mRNA (counts per million) levels are unchanged at 4-cell stage and morula stage when cultured in –G condition.
(**B', C'**) –G (**C'**) grown embryos do not incorporate decreased amounts of EU, which marks synthesis of nascent transcripts, compared embryos grown in +G medium (**B'**).

(**D'-G'**) In control medium TEAD4 protein (red) is expressed in the nuclei of all blastomeres at morula stage (78h) (**D'**). This expression is lost in embryos grown in –G medium (**E'**). Quantitation of TEAD4 protein level shown in (**F'**). (**G'**) *Tead4* mRNA (counts per million) levels are significantly reduced, at the compacted 8-cell stage, in embryos grown in –G medium.

Figure S5. Activation of mTOR by glucose and S1P, related to Figure 6.

Embryos were isolated at 18h and cultured in either +G or –G media until 78h, and inhibitors were added to the medium at 50h. Cell membranes are marked by phalloidin-FITC staining (green).

(**A-D**) mTOR target expression requires glucose. In control embryos high levels of pS757-ULK1 (**A**) or pS236-RPS6 (**C**) are seen at 78h. Embryos cultured in –G medium show a dramatic decrease in the levels of pS757-ULK1 (**B**) and pS236-RPS6 (**D**).

(**E-H**) CDX2 expression is lost upon mTOR inhibition with Torin2 (**F**) and INK128 (**G**) and inhibition of S1P signaling by JTE-013 (**H**).

(**I-P**) Inhibition of mTORC1 and S1P signaling does not perturb OCT4 and YAP1 expression. mTOR inhibition with Torin2 (**J, N**) and INK128 (**K, O**) and S1P signaling by JTE-013 (**L, P**) does not affect OCT4 (**I-L**) and YAP1 (**M-P**).

(**Q-T**) Inhibition of purine synthesis decreases TFAP2C expression. The expression of TFAP2C is eliminated in the presence of purine synthesis inhibitors, lometrexol (LTX, **Q**), methotrexate (MTX, **R**), mizoribine (Miz, **S**) and AVN-944 (**T**).

(**U-X**) Inhibition of purine synthesis does not perturb YAP1 expression. Purine synthesis inhibition with LTX (**U**), MTX (**V**), Miz (**W**) and AVN-944 (**X**) does not affect YAP1.

(**Y**) Quantitation of TFAP2C expression in embryos in which the purine synthesis is inhibited.

(**Z**) Quantitation of phosphorylation of 4E-BP1 in embryos in which the mTOR and S1P pathways are inhibited (the control data are shared with Figure 6D).